Title
Robust SERS spectral analysis for quantitative detection of pycocyanin in biological fluids

ISBN
978-1-5106-1161-0

Authors
Nguyen, Cuong
Thrift, Will
Bhattacharjee, Arunima
et al.

Publication Date
2017

DOI
10.1117/12.2267958

Robust SERS spectral analysis for quantitative detection of pyocyanin in biological fluids

Cuong Nguyen[a], Will Thrift[a], Arunima Bhattacharjee[a], Katrine Whiteson[b], Allon Hochbaum[a], Regina Ragan[a]

[a] Department of Chemical Engineering and Materials Science, University of California, Irvine, Irvine, California 92697, United States; [b] Department of Molecular Biology and Biochemistry, University of California, Irvine, Irvine, California 92697, United States

ABSTRACT

We demonstrate the advantage of using machine learning for surface enhanced Raman scattering (SERS) spectral analysis for quantitative detection of pyocyanin in Luria-Bertani media. Planar Au nanoparticle clusters were self-assembled on PS-b-PMMA diblock copolymer template using EDC crosslinking chemistry and electrohydrodynamic flow to fabricate SERS substrates. Resulting substrates produce uniform SERS response over large area with signal relative standard deviation of 10.8 % over 50 μm x 50 μm region. Taking advantage of the uniformity, 400 SERS spectra were collected at each pyocyanin concentration as training dataset. Tracking the intensity of pyocyanin 1350 cm^{-1} vibrational band shows linear regime beginning at 10 ppb. PLS analysis was also performed on the same training dataset. Without being explicitly "told" which spectrum to look for, PLS analysis recognizes the SERS spectrum of pyocyanin as its first loading vector even in the presence of other molecules in LB media. PLS regression enables quantitative detection at 1 ppb, 1 order of magnitude earlier than univariate regression. We hope this work will fuel a push toward wider adoption of more sophisticated machine learning algorithms for quantitative analysis of SERS spectra.

Keywords: self-assembly, surface enhanced Raman scattering, metabolomics, machine learning, colloidal assembly, plasmonics, biosensing

1. INTRODUCTION

Surface enhanced Raman scattering (SERS) spectroscopy is a powerful surface enhanced vibrational spectroscopic technique[1,2] that can reach sub-nanomolar detection limit[3–6]. Small detection limits are achieved by increasing the electric field in the vicinity of analyte molecules $|E_{loc}|$ – the observed SERS signal scales by a momentous $|E_{loc}|^4$.[7] Ultralarge field enhancements are usually achieved by taking advantage of the localized surface plasmon resonance (LSPR) exhibited by metal nanostructures. To date, the largest field enhancements have been achieved by "hotspots", nanogaps between metal nanostructures. Single nanometer scale hotspots have led to SERS enhancement factors (EF) ($EF \propto |E_{loc}|^4$) greater than 10^9.[8] SERS has found wide adoption in the fields of biosensing,[9–12] revealing hitherto unknown molecular signaling.[13]

Vibrational spectroscopies, like SERS, interrogate the diverse array of vibrations that a single molecule exhibits, providing a "molecular fingerprint" that allows for similar molecules to be differentiated. However, while SERS provides extensive vibrational information on the analyte, traditionally quantitative SERS spectral analysis has been carried out with single vibrational band.[14–17] This excludes the rich vibrational information contained in SERS spectra and leads to artifacts caused by the location-dependent enhancement that the analyte molecule experiences.

With the rise in computing power, it is now possible to process and manipulate large datasets with a personal computer. This allows for sophisticated machine learning algorithms to be used in quantitative spectral analysis. Partial least squares (PLS) analysis is a powerful tool that can improve quantitative detection in SERS due to its ability to decompose spectra into loading vectors that represent the most variances in analyte concentration.[18]

Biosensing and Nanomedicine X, edited by Hooman Mohseni, Massoud H. Agahi, Manijeh Razeghi,
Proc. of SPIE Vol. 10352, 1035205 · © 2017 SPIE · CCC code: 0277-786X/17/$18 · doi: 10.1117/12.2267958

An important aspect of machine learning is the training data, spectra taken at a known concentration that are used to construct the predictive model. Spectra need to be reliable, yet diverse enough to be robust to variations observed in realistic experiments. SERS experiments rely on metal nanostructures, this inherently convolves concentration of analyte with the field enhancement produced by the structures.[19] Therefore, it is essential to minimize variations in field enhancement. Yet, hotspots are inherently deeply subdiffractive, making SERS substrates challenging to fabricate in a reproducible way. By utilizing electrohydrodynamic flow enabled EDC crosslinking chemistry, SERS substrates are fabricated with an average enhancement factor (EF) greater than 10^9,[20] with signal relative standard deviation of approximately 10.8% over 50 μm x 50 μm area. This uniformity enables the collection of large numbers of training spectra, which greatly improve predictive outcomes.

In this paper, we demonstrate advantages of PLS analysis over univariate analysis in quantifying analytes with SERS in the presence of contaminants. Pyocyanin, an important quorum sensing compounds of *Pseudomonas Aeruginosa* (PA), is used as the analyte. PA commonly infects immunocompromised individuals, such as those with cystic fibrosis, HIV/AIDS, and open wounds/burns. The treatment of these chronic infections has led to antibiotic resistance in PA, a serious public health crisis. Thus, detecting and quantifying low concentrations of pyocyanin can improve the current antibiotic treatment procedures. When tracking single vibrational band, 10 ppb quantitative detection is achieved, a remarkable sensing performance. However, from the same set of training spectra, PLS analysis can start quantifying pyocyanin at 1 ppb, gaining an order of magnitude in quantification limit. While modest, an order of magnitude increase in the quantification limit can be the difference between life and death. This work, in the big picture, aims at motivating researchers to utilize advancements in computing in modern data analysis, and more specifically, intends to reveal the potential of machine learning in SERS spectral analysis.

2. MATERIALS AND METHODS

2.1 Materials

Random copolymer poly(styrene-co-methyl methacrylate)-α-hydroxyl-ω-tempo moiety (PS-r-PMMA) (Mn = 7400, 59.6% PS) and block copolymer poly(styrene-b-methyl methacrylate) (PS-b-PMMA) (Mn = 260 000 (PS), 63 500 (PMMA)) were purchased from Polymer Source, Inc. (Dorval, Canada). Ethylenediamine, dimethyl sulfoxide (DMSO), ethanol, isopropanol, toluene, potassium carbonate, 1-ethyl-3-[3-dimethylaminopropyl] carbodiimide hydrochloride (EDC), N-hydroxy sulfosuccinimide (S-NHS), and 52-mesh Pt gauze foil were purchased from Sigma Aldrich (St. Louis, MO). Gold nanospheres of 40 nm in diameter with lipoic acid functionalization were purchased from Nanocomposix (San Diego, CA). Hydrofluoric acid (HF) were purchased from Fisher Scientific (Pittsburgh, PA). MES 0.1 M buffer waspurchased from Thermo Scientific Pierce Protein Research Products (Rockford, IL). Silicon (001) wafers with resistivity of 0.004 ohm-cm were purchased from Virginia Semiconductor (Frederickburg, VA). Nanopure water (18.2 MΩ cm−1) was obtained from a Milli-Q Millipore System.

2.2 SERS Surface Fabrication

PS-b-PMMA block copolymer template was prepared as described in previous work.[21,22] 1 wt% PS-r-PMMA random copolymer solution in toluene was spun coated on a HF-cleaned, heavily doped Si wafer at 3000 rpm for 45 s and annealed at 198°C for 72h in vacuum conditions followed by rinsing with toluene. 1 wt% PS-b-PMMA solution in toluene was spun coated on the rinsed surface at 3000 rpm for 45 s followed by annealing at 198°C for 72h in vacuum conditions to produce the desired PS-b-PMMA diblock copolymer template.

The PMMA regions were functionalized with amine end groups by immersing the substrate in DMSO then in ethylenediamine/DMSO solution (5% v/v) for 5 minutes each without rinsing between steps. The resulting substrate is then washed with IPA for 1 minute and dried under nitrogen.

Lipoic functionalized 40nm Au nanoparticles solution was concentrated 2-fold by adjusting the pH to 8 with potassium carbonate, centrifuging for 25 minutes at 1700 RCF, and redispersing in DI water. 3 mL of concentrated Au solution was added to a beaker, followed by 35 μL of freshly prepared 20 mM s-NHS and 8 mM EDC both in 0.1 M MES buffer; The mixture was brought to 80°C. A 1 cm x 1 cm Si substrate previously prepared and a 1 cm x 1 cm Pt mesh were placed in the solution vertically, held by alligator clips as cathode and anode, respectively. The two were parallel to each other and 5 mm apart. A DC regulated power supply was used to apply 1.2 V for 10 minutes. The substrate, Pt mesh, and beaker were rinsed with acetone and IPA for 1 minute each and dried under nitrogen. The process was repeated with the same substrate, but with 25 μL of EDC and s-NH solution.

2.3 Raman Spectroscopy

Surface enhanced Raman scattering (SERS) measurements were carried out using a Renishaw InVia Raman Microscope with a laser excitation wavelength of 785 nm. To estimate optical uniformity of fabricated substrates, SERS substrates were immersed in 10^{-3} M BZT solution in IPA for 12 h and rinsed with methanol. A 60 X water immersion objective with a 1.2 NA wetted with DI water was used to collect SERS response map. Each spectrum was acquired with 76 μW and 0.1 s.

SERS measurements were also performed on serial dilution of pyocyanin in LB media and cell-free supernatant. Same objective as above was used; however, all measurements were collected at 7.3 μW and 0.5 s. Measurements were taken from low to high over the same area on SERS surfaces.

2.4 Multivariate Data Analysis

Data processing and analysis were done in MATLAB R2016b (The MathWorks Inc, Natrick, MA). Each spectra is baseline corrected, smoothed, and normalized to the average intensity of Si second-order vibrational band. The spectra were log-transformed before analysis using partial least squares regression (PLSR). Benzenethiol's SERS spectra were baseline corrected and min-max normalized.

3. RESULTS AND DISCUSSIONS

3.1 Self-Assembly for Large Area Optical Uniformity

Template-assisted chemical self-assembly allows for discrete nanoparticle clusters to form on surfaces are employed in SERS. Here, a diblock copolymer template is used in conjunction with EDC crosslinking chemistry to fabricate SERS surfaces through a two-step deposition process. The copolymer is prepared on a Si substrate and self organizes into PMMA domains of 40 nm in width separated by PS domains; the PMMA domains are selectively functionalized with amine end groups. In the first step, carboxylic acid terminated Au nanospheres are electrophoretically driven to the copolymer surface (Figure 1a). EDC crosslinking chemistry is used to couple the carboxlic acid moieties with amine end groups on the PMMA domains, immobilizing nanoparticles via peptide bond formation. These particles serve as monomer "seeds" for cluster growth. In the second step, the applied field also leads to the generation of electrohydrodynamic (EHD) flow that drives formation of discrete nanoparticles clusters. The applied field polarizes monomer "seeds" on the copolymer surface, producing a local inhomogeneous electric field. This field drives ion flow, thus inducing osmosis that dictates the local fluid flow. The outcome is an attractive lateral flow field on the plane of the substrate electrode, termed EHD flow,[23–25] that entrains nearby nanospheres in the colloid towards the "seed" monomers (Figure 1b). Here, the transient clusters are immobilized through a different pathway of EDC crosslinking chemistry that is enabled due to the proximity of carboxylic end groups: Anhydride bridges are formed between the carboxylic acid end groups on the nanospheres, ultimately freezing the clusters in place while maintaining uniform interparticle gap spacings of approximately 0.9 nm.[20]

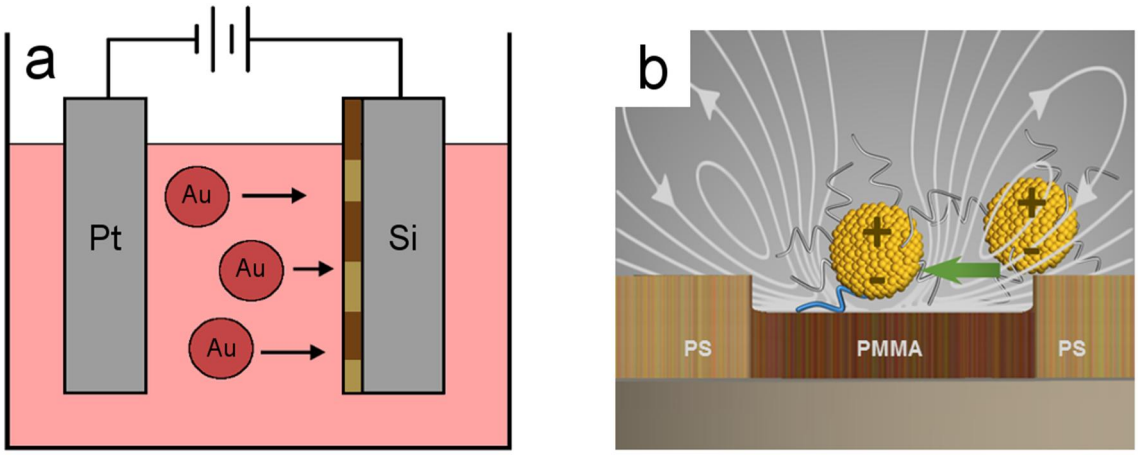

Figure 1. a) Au nanospheres are electrophoretically driven to the PS-b-PMMA template using an applied DC field. b) Electrohydrodynamic flow (light grey arrows), generated from inhomogeneous field at the electrode surface through polarization of the "seed" monomer, pushes colloidal Au nanospheres toward "seed" monomers to be immobilized through anhydride bridging.

The fabrication method allows for control over two different length scale: First is interparticle gap spacings over shorter length scale as discussed above; Second is cluster morphology over cm length scales due to the PS-b-PMMA copolymer template. The template insures that large aggregates do not form, resulting in surfaces with morphology shown in Figure 2a, where 85% of clusters have fewer than 5 particles.[26] The surface exhibits a broad absorption band from 615 nm to 875 nm that agrees well with FDTD calculations.[20]

Furthermore, controlling the two length scales allow for extremely uniform SERS response over large area. Benzenethiol (BZT), a well characterized analyte that binds to gold surfaces due to the thiol-Au interaction, was used as a standard. Map of normalized intensity at the 1071 cm^{-1} vibrational band (Figure 2b) shows relative standard deviation below 10.8% over 50 µm x 50 µm area. This uniformity enables the use of machine learning algorithms in quantitative molecular detection through the acquisition of large training dataset.

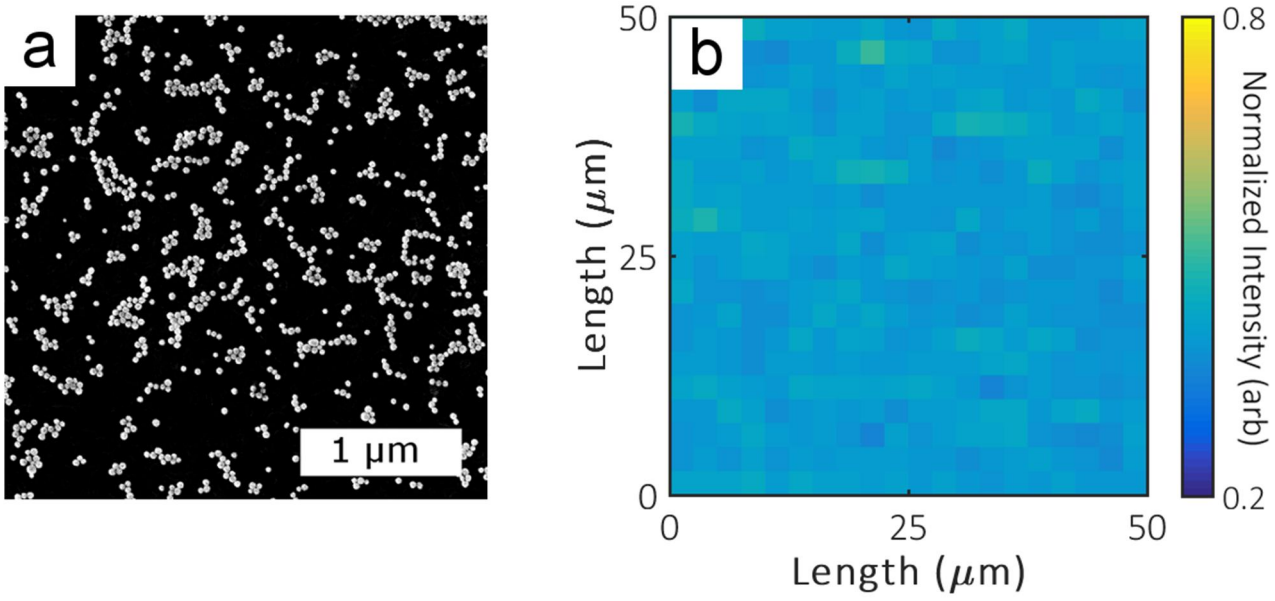

Figure 2. a) SEM image of Au clusters on SERS substrates after the two-step fabrication process. b) SERS intensity map of BZT's 1071 cm^{-1} vibrational band across a 50 µm x 50 µm area with RSD of 10.8%

3.2 Machine Learning for Improved Quantitative Label-Free Molecular Detection

While one of SERS advantages lies in its ability for label-free detection, this asset also means its performance can be hindered by other molecules. Machine learning algorithms, specifically partial least square (PLS) regression in this case, can provide better quantitative detection with SERS than tracking single vibrational band, as traditionally done with SERS. By performing PLS analysis on large training dataset, enabled by SERS substrates' uniform response, lower quantitation limit is achieved.

Here, SERS measurements were performed on serial dilutions of pyocyanin in Luria-Bertani (LB) broth, a liquid medium made up of nutrients used in culturing bacteria; 400 spectra were collected for each dilution. When tracking a single vibrational band, quantitative detection is achieved when behavior of SERS intensity can be correlated with changes in analyte concentration. SERS intensity of the pyocyanin's 1350 cm^{-1} vibrational band exhibits a linear regime between 10 ppb and 100 ppm (Figure 3), within which pyocyanin concentration can be described using the formula: $\log C = 2.55 \times \log I + 4.57$ ($R^2 = 0.98$). While this performance is remarkable, it is possible that SERS signal at lower concentrations is washed out due to signal interferences from other molecules in the broth.

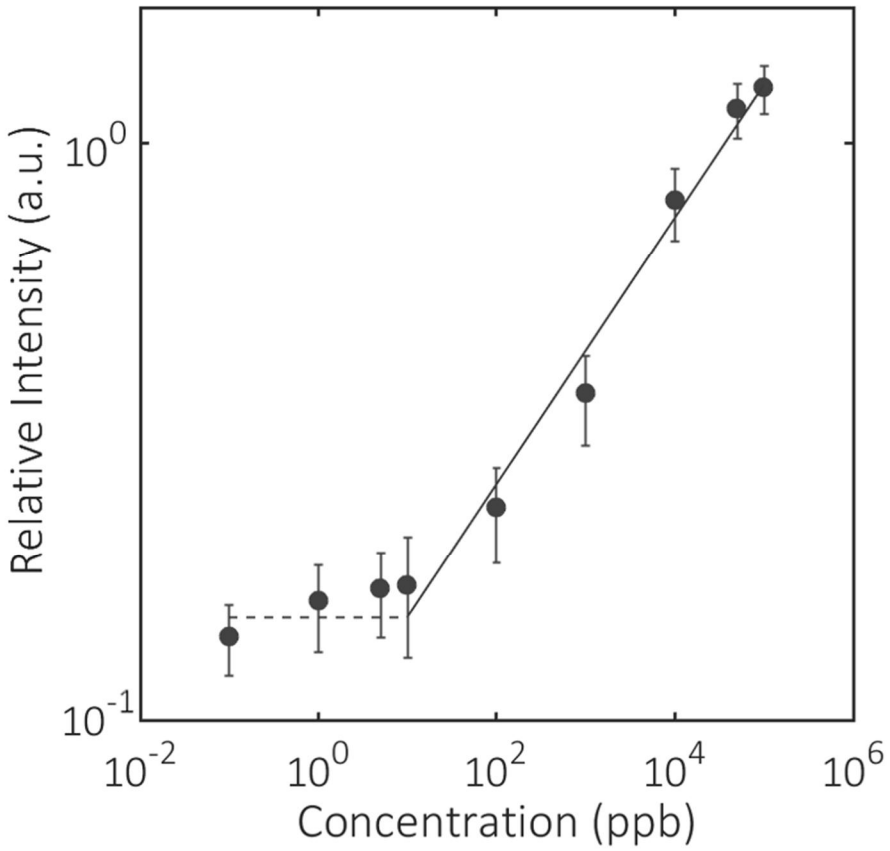

Figure 3. SERS dose-response curve of pyocyanin's 1350 cm^{-1} vibrational band. Solid line indicates linear regime where quantitation can be achieved.

To address this, an analysis that accounts for information in the whole spectra is needed. In the simplest terms, this analysis should be able to create a model that predicts pyocyanin concentration (observation), from a vector of intensity values (predictors), i.e. a spectrum. From first glance, this goal can be accomplished using ordinary multiple linear regression. However, the classic problem of collinearity exists in this case as values in a spectrum are correlated to each other, resulting in redundancy in the regression analysis. Many solution to this problem exist. One of such is principal component analysis,[27] where the matrix of training spectra is rotated and scaled and decomposed into its principal components such that the first principal component accounts for the most variance in the dataset and so on; these components are then used in ordinary multiple regression. In this case, although the problem of collinearity is eliminated

by the orthogonality of the components, a different issue of choosing the optimal components arises. With PLS, both the matrix of training spectra and concentration are decomposed into components that account for each other, rather than just the training spectra as in the case of PCA.[28] When the decomposition is carried out properly, the first component, or loading vector, should explain the most variance in the concentration vector.[29] The number of loading vectors is chosen based on the minimal amount required for accurate prediction.[28] This is done by performing cross validation on the model while varying the number of components uses; A minimum in RMSE cross validation (RMSECV) indicates the optimal number of components. Ordinary multiple regression is then performed on the loading vectors.

PLS analysis was performed on the same set of spectra as above. From the 400 spectra collected per dilution, 380 spectra are randomly selected as the training set, and 20 are withheld as the testing set. 10 loading vectors, where RMSECV is minimized (Figure 3b inset), were used to create the predictive model. Testing the model with the 20 withheld spectra shows accurate quantification capabilities between 1 ppb and 10 ppm; Fitting a y = x line, representing perfect predictions, gives R^2 = 0.931 (Figure 2b). It must be noted here that PLS regression improves quantitative detection limit by 1 order of magnitude in concentration in comparison to univariate linear regression on a single vibrational band. This is because PLS analysis decomposes spectra into loading vectors that can explain changes in concentration and discards the redundant and irrelevant spectral information through loading vectors selection process. Consequently, the first loading vector represents almost perfectly the SERS spectra of pyocyanin in DI water, although the algorithm was never explicitly "told" to look for pyocyanin vibrational bands (Figure 3c).

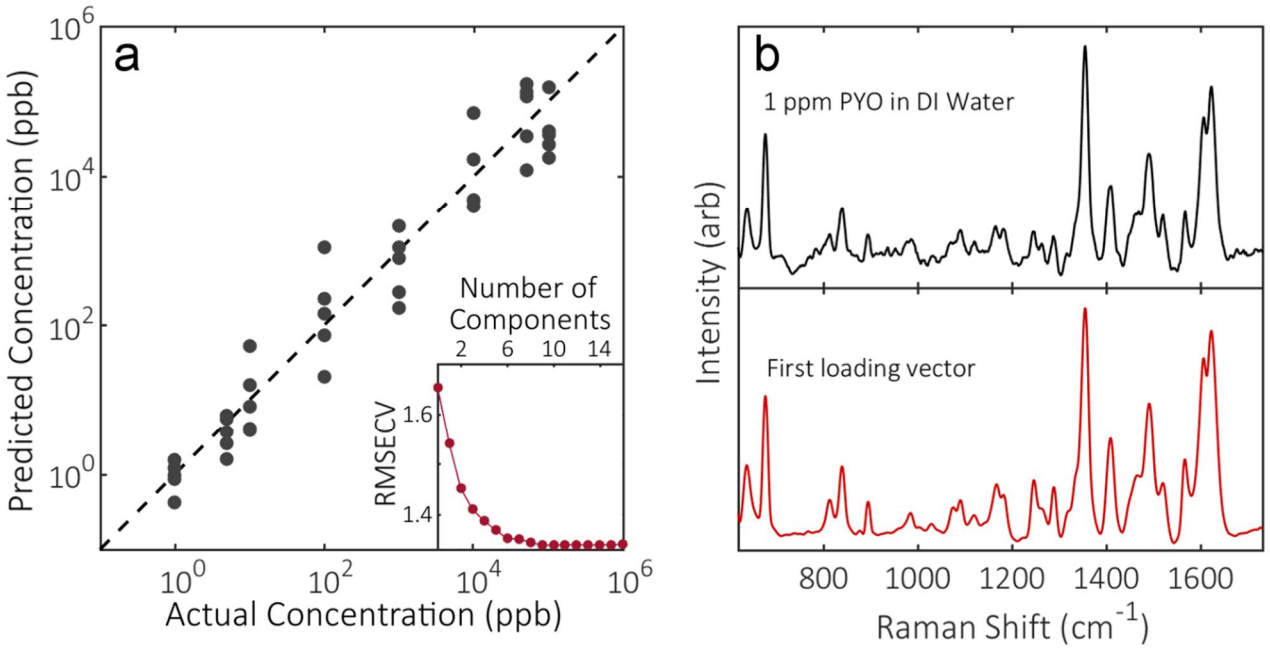

Figure 4. a) Pyocyanin concentration predicted by PLS model for testing spectra plotted against their actual concentrations. Dashed line (y = x) represents perfect predictive capability. Inset: Root-mean-squared error of cross validation as a function of number of PLS components used in the model. b) Top: SERS spectrum of 1 ppm pyocyanin in DI water. Bottom: First loading vector extracted from PLS model. Note that pyocyanin's major vibrational bands can be identified in the loading vector.

While PLS analysis demonstrates definite improvements in SERS spectral analysis, it also comes with disadvantages, mainly the fact that it is a linear model. SERS spectral response to changes in analyte concentration, although can be approximated, or log-transformed as we have done here, to be linear in some cases, are more accurately represented by a non-linear model. In the future, more advanced machine learning algorithms, namely artificial neural networks (ANN), can be used. ANN is a bioinspired algorithm that can model non-linear system and has been demonstrated to work well in SERS spectral analysis.

4. CONCLUSION

In this work, we have demonstrated the benefits and use of machine learning, particularly PLS regression in SERS spectral analysis for quantitative molecular detection. Self-assembly of Au nanoparticle clusters utilizing EDC crosslinking chemistry and EHD flow on PS-b-PMMA chemical template produces SERS substrates with high uniformity over large area – suitable to generate large training datasets. PLS regression allows for quantitative detection of pyocyanin starting 1 ppb, an order of magnitude earlier than univariate regression on intensity of pyocyanin's 1350 cm^{-1} vibrational band. Future work may involve using more advanced machine learning algorithms such as ANN to perform multiplex assays.

REFERENCES

[1] Kneipp, K., Moskovits, M. and Kneipp, H., eds., [Surface-Enhanced Raman Scattering], Springer Berlin Heidelberg (2006).

[2] Le Ru, E. C. and Etchegoin, P. G., "EM enhancements and plasmon resonances: examples and discussion," [Principles of Surface-Enhanced Raman Spectroscopy], Elsevier, Amsterdam, 299–365 (2009).

[3] Fan, W., Hong Lee, Y., Pedireddy, S., Zhang, Q., Liu, T. and Yi Ling, X., "Graphene oxide and shape-controlled silver nanoparticle hybrids for ultrasensitive single-particle surface-enhanced Raman scattering (SERS) sensing," Nanoscale **6**(9), 4843–4851 (2014).

[4] Ganbold, E.-O., Min Lee, C., Cho, E.-M., Jun Son, S., Kim, S., Joo, S.-W. and Ik Yang, S., "Subnanomolar detection of ochratoxin A using aptamer-attached silver nanoparticles and surface-enhanced Raman scattering," Anal. Methods **6**(11), 3573–3577 (2014).

[5] Sharma, V., Kumar, S., Jaiswal, A. and Krishnan, V., "Gold Deposited Plant Leaves for SERS: Role of Surface Morphology, Wettability and Deposition Technique in Determining the Enhancement Factor and Sensitivity of Detection," ChemistrySelect **2**(1), 165–174 (2017).

[6] Patze, S., Huebner, U., Liebold, F., Weber, K., Cialla-May, D. and Popp, J., "SERS as an analytical tool in environmental science: The detection of sulfamethoxazole in the nanomolar range by applying a microfluidic cartridge setup," Anal. Chim. Acta **949**(Supplement C), 1–7 (2017).

[7] Kerker, M., Wang, D.-S. and Chew, H., "Surface enhanced Raman scattering (SERS) by molecules adsorbed at spherical particles," Appl. Opt. **19**(19), 3373 (1980).

[8] Lim, D.-K., Jeon, K.-S., Hwang, J.-H., Kim, H., Kwon, S., Suh, Y. D. and Nam, J.-M., "Highly uniform and reproducible surface-enhanced Raman scattering from DNA-tailorable nanoparticles with 1-nm interior gap," Nat. Nanotechnol. **6**(7), 452–460 (2011).

[9] Cao, Y. C., Jin, R. and Mirkin, C. A., "Nanoparticles with Raman Spectroscopic Fingerprints for DNA and RNA Detection," Science **297**(5586), 1536–1540 (2002).

[10] Fang, C., Agarwal, A., Buddharaju, K. D., Khalid, N. M., Salim, S. M., Widjaja, E., Garland, M. V., Balasubramanian, N. and Kwong, D.-L., "DNA detection using nanostructured SERS substrates with Rhodamine B as Raman label," Biosens. Bioelectron. **24**(2), 216–221 (2008).

[11] Guerrini, L., Arenal, R., Mannini, B., Chiti, F., Pini, R., Matteini, P. and Alvarez-Puebla, R. A., "SERS Detection of Amyloid Oligomers on Metallorganic-Decorated Plasmonic Beads," ACS Appl. Mater. Interfaces **7**(18), 9420–9428 (2015).

[12] Costas, C., López-Puente, V., Bodelón, G., González-Bello, C., Pérez-Juste, J., Pastoriza-Santos, I. and Liz-Marzán, L. M., "Using Surface Enhanced Raman Scattering to Analyze the Interactions of Protein Receptors with Bacterial Quorum Sensing Modulators," ACS Nano **9**(5), 5567–5576 (2015).

[13] Bodelón, G., Montes-García, V., López-Puente, V., Hill, E. H., Hamon, C., Sanz-Ortiz, M. N., Rodal-Cedeira, S., Costas, C., Celiksoy, S., Pérez-Juste, I., Scarabelli, L., La Porta, A., Pérez-Juste, J., Pastoriza-Santos, I. and Liz-Marzán, L. M., "Detection and imaging of quorum sensing in Pseudomonas aeruginosa biofilm communities by surface-enhanced resonance Raman scattering," Nat. Mater. **15**(11), 1203–1211 (2016).

[14] Grubisha, D. S., Lipert, R. J., Park, H.-Y., Driskell, J. and Porter, M. D., "Femtomolar Detection of Prostate-Specific Antigen: An Immunoassay Based on Surface-Enhanced Raman Scattering and Immunogold Labels," Anal. Chem. **75**(21), 5936–5943 (2003).

[15] Wu, X., Chen, J., Li, X., Zhao, Y. and Zughaier, S. M., "Culture-free diagnostics of Pseudomonas aeruginosa infection by silver nanorod array based SERS from clinical sputum samples," Nanomedicine Nanotechnol. Biol. Med. **10**(8), 1863–1870 (2014).

[16] Qi, G., Jia, K., Fu, C., Xu, S. and Xu, W., "A highly sensitive SERS sensor for quantitative analysis of glucose based on the chemical etching of silver nanoparticles," J. Opt. **17**(11), 114020 (2015).
[17] Srichan, C., Ekpanyapong, M., Horprathum, M., Eiamchai, P., Nuntawong, N., Phokharatkul, D., Danvirutai, P., Bohez, E., Wisitsoraat, A. and Tuantranont, A., "Highly-Sensitive Surface-Enhanced Raman Spectroscopy (SERS)-based Chemical Sensor using 3D Graphene Foam Decorated with Silver Nanoparticles as SERS substrate," Sci. Rep. **6**, 23733 (2016).
[18] Geladi, P. and Kowalski, B. R., "Partial least-squares regression: a tutorial," Anal. Chim. Acta **185**, 1–17 (1986).
[19] Fang, Y., Seong, N.-H. and Dlott, D. D., "Measurement of the Distribution of Site Enhancements in Surface-Enhanced Raman Scattering," Science **321**(5887), 388–392 (2008).
[20] Thrift, W., Nguyen, C., Darvishzadeh-Varcheie, M., Zare, S., Sharac, N., Sanderson, R., Dupper, T., Hochbaum, A., Capolino, F., Qomi, M. J. A. and Ragan, R., "Driving Chemical Reactions in Plasmonic Nanogaps with Electrohydrodynamic Flow," ACS Nano Submitt.
[21] Adams, S. M., Campione, S., Caldwell, J. D., Bezares, F. J., Culbertson, J. C., Capolino, F. and Ragan, R., "Non-lithographic SERS Substrates: Tailoring Surface Chemistry for Au Nanoparticle Cluster Assembly," Small **8**(14), 2239–2249 (2012).
[22] Adams, S. M., Campione, S., Capolino, F. and Ragan, R., "Directing Cluster Formation of Au Nanoparticles from Colloidal Solution," Langmuir **29**(13), 4242–4251 (2013).
[23] Trau, M., Saville, D. A. and Aksay, I. A., "Assembly of Colloidal Crystals at Electrode Interfaces," Langmuir **13**(24), 6375–6381 (1997).
[24] Sides, P. J., "Electrohydrodynamic Particle Aggregation on an Electrode Driven by an Alternating Electric Field Normal to It," Langmuir **17**(19), 5791–5800 (2001).
[25] Ristenpart, W. D., Jiang, P., Slowik, M. A., Punckt, C., Saville, D. A. and Aksay, I. A., "Electrohydrodynamic Flow and Colloidal Patterning near Inhomogeneities on Electrodes," Langmuir **24**(21), 12172–12180 (2008).
[26] Thrift, W., Bhattacharjee, A., Darvishzadeh-Varcheie, M., Lu, Y., Hochbaum, A., Capolino, F., Whiteson, K. and Ragan, R., "Surface enhanced Raman scattering for detection of Pseudomonas aeruginosa quorum sensing compounds," Biosensing Nanomedicine VIII **9550**, 95500B–95500B–13 (2015).
[27] Wold, S., Esbensen, K. and Geladi, P., "Principal component analysis," Chemom. Intell. Lab. Syst. **2**(1), 37–52 (1987).
[28] Höskuldsson, A., "PLS regression methods," J. Chemom. **2**(3), 211–228 (1988).
[29] Wold, S., Sjöström, M. and Eriksson, L., "PLS-regression: a basic tool of chemometrics," Chemom. Intell. Lab. Syst. **58**(2), 109–130 (2001).